APPLIED AND ENVIRONMENTAL MICROBIOLOGY, Aug. 1986, p. 281–289
0099-2240/86/080281-09$02.00/0

Vol. 52, No. 2

Inhibitor Studies of Dissimilative Fe(III) Reduction by *Pseudomonas* sp. Strain 200 ("*Pseudomonas ferrireductans*")

ROBERT G. ARNOLD, THOMAS J. DiCHRISTINA, AND MICHAEL R. HOFFMANN*
California Institute of Technology, W. M. Keck Laboratories, Pasadena, California 91125

Received 21 February 1986/Accepted 7 May 1986

Aerobic respiration and dissimilative iron reduction were studied in pure, batch cultures of *Pseudomonas* sp. strain 200 ("*Pseudomonas ferrireductans*"). Specific respiratory inhibitors were used to identify elements of electron transport chains involved in the reduction of molecular oxygen and Fe(III). When cells were grown at a high oxygen concentration, dissimilative iron reduction occurred via an abbreviated electron transport chain. The induction of alternative respiratory pathways resulted from growth at low oxygen tension (<0.01 atm [1 atm = 101.29 kPa]). Induced cells were capable of O_2 utilization at moderately increased rates; dissimilative iron reduction was accelerated by a factor of 6 to 8. In cells grown at low oxygen tension, dissimilative iron reduction appeared to be uncoupled from oxidative phosphorylation. Models of induced and uninduced electron transport chains, including a mathematical treatment of chemical inhibition within the uninduced, aerobic electron transport system, are presented. In uninduced cells respiring anaerobically, electron transport was limited by ferrireductase activity. This limitation may disappear among induced cells.

The chemiosmotic hypothesis of Mitchell (16, 17) states that electron transport is coupled to oxidative phosphorylation by the following mechanism. Reducing equivalents enter the respiratory chain via one of several dehydrogenases (often flavin-containing enzymes, e.g., NADH and succinate dehydrogenases) and are passed sequentially down a chain of carriers which includes iron-sulfur proteins, coenzyme Q, and a series of cytochromes (9). In mitochondria, molecular oxygen serves as the final electron acceptor. Energy available from electron transport supports an electrochemical proton motive force which drives ADP phosphorylation (coupled to proton retranslocation via membrane-bound ATPase).

Similarities between mitochondrial and bacterial respiration have prompted speculation that mitochondria originated as bacterial endosymbionts (9) or fragments of specialized bacterial membranes (24). However, there are fundamental differences in bacterial systems, including the following: (i) species- and strain-dependent variations in transport chain composition; (ii) intrastrain dependence of transport chain composition on growth conditions; (iii) the branched nature of bacterial respiratory systems, which provides a measure of metabolic flexibility absent in their mitochondrial counterpart (25, 31); (iv) their respective H^+/ATP ratios (11) (despite the similarities [3] between mitochondrial and bacterial membrane-bound ATPases); and (v) structural differences between mitochondrial and bacterial cytochrome oxidases, including aa_3-type oxidases (24). Bacterial respiration can terminate with a number of electron acceptors, including O_2, NO_3^-, NO_2^-, SO_3^{2-}, SO_4^{2-}, and Fe(III) (10). The development of alternative electron transport pathways is often inducible in the absence of more thermodynamically favorable routes.

Pseudomonas sp. strain 200 (hereinafter referred to as "*Pseudomonas ferrireductans*") is capable of catalyzing dissimilative iron reduction [Fe(III) + $e^- \rightarrow$ Fe(II)] at rates considerably higher than those reported for other capable bacteria, e.g., *Thiobacillus thiooxidans* (2, 12), *Bacillus circulans* (29, 30), *Bacillus polymyxa* (19), and *Clostridium butyricum* (19). Previous experiments in this laboratory showed that electron transport to Fe(III) can proceed at a rate comparable to that observed during aerobic respiration (R. G. Arnold, T. M. Olson, and M. R. Hoffmann, Biotechnol. Bioeng., in press). Iron reduction activity in "*P. ferrireductans*" is known to respond to growth medium composition. Furthermore, Fe(III) reduction is directly related to cell pigmentation and can be inhibited by HOQNO (2-heptyl-4-hydroxyquinoline *N*-oxide) (Sigma Chemical Co.) (20, 21; C. O. Obuekwe, Ph.D. dissertation, University of Alberta, Edmonton, Alberta, Canada, 1980). The cytochrome content is directly correlated with ferrireductase activity.

A variety of reagents are known to interfere with electron transport. When the site or mechanism of electron transport inhibition is known, inhibitor studies offer insights into the character of the electron transport chain and the identities of individual electron carriers (7). However, respiratory inhibitors frequently act at more than one site (14).

Kinetic data for oxygen utilization and Fe(III) reduction by "*P. ferrireductans*" are reported here. These data are used to (i) identify (and contrast) electron carriers involved in aerobic respiration versus dissimilative iron reduction, (ii) identify inducible elements of the electron transport chain, (iii) support models of electron transport kinetics and inhibitor activity, and (iv) determine whether dissimilative iron reduction can support oxidative phosphorylation.

MATERIALS AND METHODS

Four types of experiments were conducted. Dissolved-oxygen utilization was monitored in uninduced and induced cultures of "*P. ferrireductans*" which differed only in the dissolved-oxygen concentration maintained during aerobic growth (see below). Similarly, dissimilative iron reduction was examined under anaerobic conditions in uninduced and induced cultures.

Aerobic respiration in uninduced cells. Oxygen utilization experiments were conducted in a 2-liter Biostat M batch reactor (Braun Instrument Co.) with automatic temperature (±0.2°C) and pH (±0.05) control (pH-stat.). Dissolved-oxygen concentration was measured continuously by using

* Corresponding author.

TABLE 1. Respiration-inhibiting chemicals used[a]

Chemical inhibitor	Concn range (M)	Solvent	Inhibition site or action	Reference(s)
Rotenone	1×10^{-5}–5×10^{-3}	Acetone	NADH dehydrogenase	6
Quinacrine dihydrochloride	1×10^{-6}–4×10^{-3}	H_2O	Flavins (dehydrogenases)	32,33
Dicumarol	1×10^{-6}–5×10^{-5}	Pyridine	Quinones	4
HOQNO	6×10^{-7}–5×10^{-5}	Ethanol	Cytochrome *b*	Obuekwe, Ph.D dissertation
NaCN	1×10^{-5}–3×10^{-3}	H_2O	Cytochrome oxidase	8, 26
NaN_3	1×10^{-5}–2×10^{-2}	H_2O	Cytochrome oxidase	8, 26
DCCD[b]	1×10^{-6}–1×10^{-4}	Acetone	F_0 subunit of ATPase (blocks oxidative phosphorylation)	3
DNP[c]	1×10^{-6}–5×10^{-4}	Acetone	Uncoupler (renders cytoplasmic membrane permeable to H^+)	6, 15, 18
Chloramphenicol[d]	2×10^{-4}–5×10^{-4}	Ethanol	Bacteriostatic agent (blocks protein synthesis)	22, 23

[a] Inhibitors were dissolved in as little solvent as possible to minimize the chances of secondary effects attributable to solvent addition. Controls were run to ensure that solvents were not themselves inhibitory at levels added.

[b] DCCD blocks proton retranslocation by binding specifically to the F_0 subunit of membrane-bound ATPase. Inhibition follows owing to proton motive back pressure.

[c] DNP uncouples electron transport from oxidative phosphorylation by rendering the cytoplasmic membrane permeable to hydrogen ions and thereby dissipating the proton motive force.

[d] Preliminary experiments (not shown) indicated that chloramphenicol addition to 0.46 mM did not impede dissimilative iron reduction. A minor, temporary reduction in O_2 utilization rate was observed, however.

an O_2 probe (type 82; Ingold Co.) fitted through the head plate of the Biostat M. In a typical experiment, the reactor was filled with 1.5 liters of lactate medium (20) (per liter: 0.5 g of K_2HPO_4, 2.0 g of Na_2SO_4, 1.0 g of NH_4Cl, 0.15 g of $CaCl_2$, 0.1 g of $MgSO_4 \cdot 7H_2O$, 0.5 g of yeast extract, 3 ml of 60% sodium lactate syrup) and autoclaved at 121°C for 30 to 60 min. Iron was added to a final concentration of 72 μM from a filter-sterilized $FeCl_3$ solution to satisfy microbial nutritional requirements. Aerobic growth was initiated by adding approximately 1.5 ml from a dense overnight culture (identical medium) of "*P. ferrireductans*." Species characteristics were summarized previously (Arnold et al., in press). Gas flow ($Q_{air} \cong 0.5$ liters/min) and mechanical agitation (250 rpm) provided mixing energy, and the temperature was maintained at 31°C. Dissolved-oxygen concentration remained at or above 80% of saturation throughout aerobic growth.

Microbial growth was monitored by periodic measurement of A_{600}. At a target optical density of 0.10 cm^{-1}, the air supply to the culture was cut off and the agitation speed was reduced to 150 rpm to minimize entrainment of air from the culture headspace while still providing mixing energy. The concentration of dissolved oxygen was measured at 15-s intervals before and after the addition of chloramphenicol (Sigma Chemical Co.) to 0.23 mM; when a steady rate of O_2 depletion was observed, inhibitor addition was initiated. Thereafter, the concentration of the inhibitor was increased periodically, with continuous monitoring of the O_2 concentration. There was sufficient time between successive additions to establish a steady oxygen utilization rate at each inhibitor concentration. A list of chemical inhibitors, concentration ranges, probable inhibition sites, and inhibitor solvents is provided in Table 1.

Aerobic respiration in induced cells. The procedures were essentially the same as those described above. However, the cultures were grown to $A_{600} = 0.25$ cm^{-1}, while dissolved oxygen was maintained at ≤2% of the saturation level. At the target optical density, chloramphenicol was added to 0.46 mM and profiles of dissolved-oxygen concentration versus time were generated at preselected inhibitor levels.

Dissimilative iron reduction in uninduced cells. "*P. ferrireductans*" was grown aerobically (dissolved-oxygen concentration, ≥0.8 of saturation level) to a target optical density of $A_{600} = 0.25$ cm^{-1}, which was chosen to provide an appreciable base-line iron reduction rate. At that point, the O_2 utilization rate was measured before and after the addition of chloramphenicol to 0.46 mM. The culture was then purged of residual oxygen with gaseous N_2, and nitrilotriacetic acid and $FeCl_3$ were added to final concentrations of 1.86×10^{-3} M. Thermodynamic calculations indicate that nitrilotriacetic acid substantially increases the overall solubility of Fe(III) (Arnold et al., in press); the rate of dissimilative iron reduction by "*P. ferrireductans*" is also increased dramatically. Samples (120 ml) were immediately transferred from the Biostat M into 250-ml flasks in a water bath shaker (31°C). The flasks were continuously purged with high-purity nitrogen gas. Respiratory inhibitors were added to preselected concentrations ranging over at least 2 orders of magnitude. The highest concentration was reserved for the Biostat M, in which pH changes due to the inhibitor addition were offset. One flask was used as a control (no inhibitor). Thereafter, reaction flasks and the Biostat M were periodically sampled for determination of total ferrous iron concentration. During the iron reduction period, pH control in the Biostat M was terminated, because similar control in the flasks was not feasible. The culture remained in the neutral pH range throughout, drifting ≤0.3 pH units.

Iron reduction in induced cells. Preliminary experiments (Fig. 1) showed that iron reduction activity in cultures of "*P. ferrireductans*" was enhanced by growth under O_2-limited conditions. Experiments were undertaken to see whether

inducible and constitutive iron reductases could be differentiated on the basis of a response to chemical inhibition. The procedures were identical to those of the iron reduction experiments described above, except that dissolved-oxygen levels were maintained at less than 2% saturation during the aerobic growth period (to A_{600} = 0.25 cm^{-1}) preceding iron addition.

Carbon monoxide inhibition. Carbon monoxide inhibition experiments represent a special case, since inhibitor concentration was not measured and could not be varied systematically. CO inhibition of dissimilative iron reduction was tested in induced and uninduced cultures grown to A_{600} = 0.25 cm^{-1} in the Biostat M.

Whole cell spectra. "*P. ferrireductans*" was grown in complex lactate medium to A_{600} = 0.75 cm^{-1} at high and low O_2 concentrations (as described above). Cells were harvested by centrifugation for 30 min at 3,000 × *g* (4°C) in a Sorvall model RC-3B centrifuge, washed, and suspended to 2% of the original volume in cold saline solution (0.15 M NaCl; 1 mM $MgCl_2$). Dithionite-reduced-minus-oxidized spectra were obtained with a Shimadzu recording spectrophotometer (model MPS-2000); cuvettes of path length 1 cm were positioned adjacent to the photomultiplier. The oxidized sample was prepared by bubbling pure O_2 through the suspension; reduced conditions were induced by the addition of a few grains of sodium dithionite ($Na_2S_2O_4$; Sigma).

Analytical procedures. Optical density (an indication of cell density) was measured with a Beckman model DU7 spectrophotometer at 600 nm and a reduced-volume cuvette with a path length of 1 cm.

To eliminate the possibility of Fe(II) autoxidation (13) after sample removal, 1 ml of anaerobic fermentation medium was rapidly added (within 5 s of sample withdrawal) to a quenching medium consisting of 0.5% (wt/vol) 1,10-phenanthroline (sufficient volume to provide excess phenanthroline) and 2 ml of ammonium acetate buffer (1). (Phenanthroline is itself a potent inhibitor [7] of electron transport.) After the addition of 50 μl of a 2 M NH_4F solution to mask the color produced by complexed Fe(III) (28), the samples were diluted to 10 ml with distilled water and centrifuged at 3,000 × *g* for 20 to 30 min in a Sorvall model RC-3B centrifuge. The centrate color was immediately assayed spectrophotometrically at 510 nm. Preliminary work in this laboratory showed that the extinction coefficient, ε_{510}, for the Fe(II)-(phenanthroline)$_3$ complex was 1.11 × 10^4 M^{-1} cm^{-1}.

Inhibitor description. Relevant information pertaining to individual chemical inhibitors is summarized in Table 1. (For the primary sites of inhibitor activity, see Fig. 10.)

RESULTS

O_2 utilization by uninduced cells. Two examples of profiles of O_2 concentration, [O_2], versus time are shown in Fig. 2. Points of inhibitor (sodium azide [Sigma] or quinacrine dihydrochloride [N^4-(6-chloro-2-methoxy-9-acridinyl-*N'*,*N'*,-diethyl-1,4-pentanediamine dihydrochloride)] addition correspond to discontinuities in the rate of oxygen disappearance ($-d[O_2]/dt$). Stable respiration rates were reestablished within 1 to 2 min of the addition of inhibitors. In the absence of inhibitors, oxygen utilization rates at the target optical density (A_{600} = 0.10 cm^{-1}) were approximately 5 × 10^{-4} M h^{-1}.

Oxygen utilization rates, determined at various points along the profile of [O_2] versus time, were used to calculate percent inhibition as a function of inhibitor concentration. The results are summarized in Fig. 3. The effects of *N*,*N'*-dicyclohexylcarbodiimide (DCCD) (Sigma) and 2,4 dinitrophenol (DNP) (Sigma) additions are not included because of their time-dependent mode of inhibition. The results indicate that all the inhibitors tested except rotenone (1,2,12,12a-tetrahydro-8,9-dimethoxy-2-(1-methylethenyl)-[1]benzopyrano[3,4-b]furo[2,3-h]-[1]-benzopyran-6(6H)-one) (Sigma) are capable of completely inhibiting electron transport to molecular oxygen. HOQNO was almost 1 order of magnitude more effective than dicumarol (3,3'-methylenebis[4-hydroxy-2H-1-benzypyran-2-one]) (Sigma) which was the next most potent respiratory inhibitor. With the exception of rotenone, sodium azide was the least effective; it was approximately 1 order of magnitude less potent than quinacrine dihydrochloride and almost 10^3 times less effective than HOQNO.

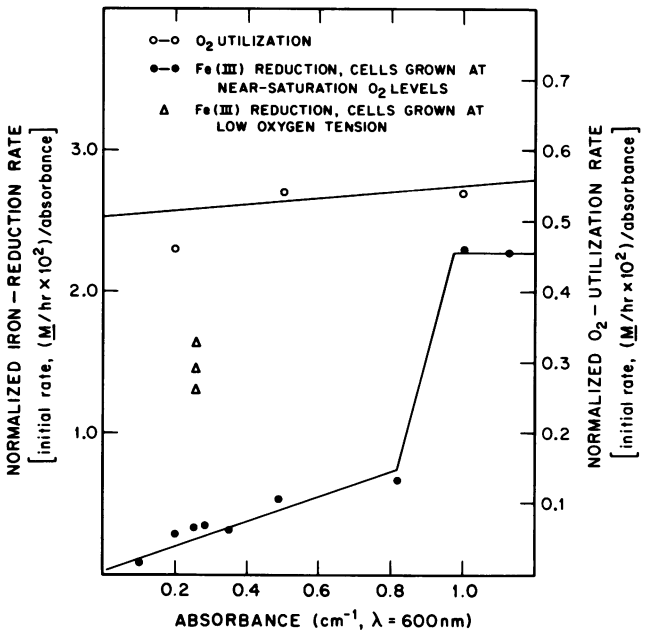

FIG. 1. Uninhibited O_2 utilization and iron reduction rates normalized on the basis of culture optical density at 600 nm.

After 40 min of exposure to 10^{-4} M DCCD, respiratory activity by "*P. ferrireductans*" was essentially zero (data not shown). Stimulation of O_2 utilization was not observed at any of the DNP levels investigated ($\geq 10^{-6}$M). Respiration was inhibited to a significant degree at DNP concentrations $\geq 10^{-4}$ M (data not shown). Cell density was much less important than DNP concentration as a determinant of inhibitor efficiency.

O_2 utilization by induced cells. Representative oxygen utilization data are also provided for induced "*P. ferrireductans*" grown at low oxygen tension (Fig. 3). It is apparent that cells grown at low oxygen concentrations are considerably less sensitive than uninduced cells to all the respiratory inhibitors tested.

Iron reduction in uninduced and induced cells. Dissimilative iron reduction in induced cells was unaffected by DCCD ($\leq 10^{-4}$ M). Among uninduced cells, both DCCD and DNP were potent inhibitors of iron reduction (although somewhat less effective than during aerobic respiration).

Examples of kinetic data for Fe(III) reduction are provided in Fig. 4. These and similar, unplotted results are summarized in dose-response curves in Fig. 5, which are similar to those generated for aerobic respiration. The effect of rotenone on dissimilative iron reduction was not tested.

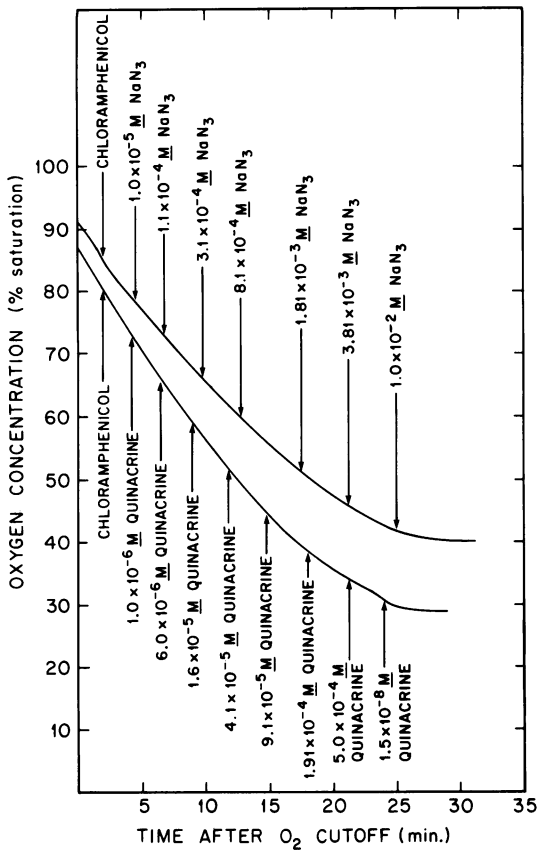

FIG. 2. Inhibition of aerobic respiration in cultures of "*P. ferrireductans*" (A_{600} = 0.10 cm^{-1}) by azide and quinacrine. Cultures were grown at near-saturation O_2 concentrations (uninduced).

A comparison of Fig. 3 and 5 indicates that, in general, the reagents used in this study are less effective inhibitors of electron transport to Fe(III) than to molecular oxygen. Neither sodium cyanide (Mallinckrodt, Inc.) nor sodium azide appeared to appreciably inhibit dissimilative iron reduction, whereas quinacrine, dicumarol, and HOQNO were all less efficient when Fe(III) was the electron acceptor.

No general trend in iron reduction inhibition is apparent from a comparison of uninduced and induced cells. When sodium cyanide or azide was present, inhibition efficiency appeared to be independent of the iron reduction competence of the cells. Although HOQNO and dicumarol were more effective among uninduced cells, the reverse was true for quinacrine inhibition.

CO inhibition in uninduced and induced cells. Constitutive iron reductase was completely inhibited by CO treatment, although the inducible system seemed unaffected.

Whole-cell spectra. Reduced-minus-oxidized spectra corresponding to induced and uninduced whole-cell suspensions are shown in Fig. 6. In both curves, strong maxima are apparent at 550 and 521 nm; there are inflections near 512 and 528 nm. In the Soret region, there is a strong peak at 420 nm and a trough at about 382 nm. Differences between the two spectra include the appearance in the induced culture of (i) elevated levels of cytochrome expression and (ii) a 630-nm peak and 646-nm trough.

DISCUSSION

Inhibition of O_2 utilization in uninduced cells. The data in Fig. 3 are consistent with the postulated mechanisms by which specific inhibitors interfere with electron transport to molecular oxygen. Assuming that (i) successive electron transfer reactions are governed by Michaelis-type kinetics and (ii) inhibitors block electron transport by binding at a single site, the kinetics of electron transport can be reduced to two simplified cases. (i) A site of inhibition is also the rate-limiting step for electron transport in the absence of an inhibitor. (ii) An inhibitor acts at a site other than the rate-limiting site or enzyme. Case (i) would hold, for example, if electron transport were limited at the dehydrogenase level and quinacrine dihydrochloride were the inhibitor or if respiration rate limits were imposed by cytochrome oxidase and the inhibition were by sodium azide or cyanide. Case (ii) would hold for all inhibitors if the uninhibited respiration rate were limited to the rate of dissipation of the proton motive force.

The mathematics of these two situations is fundamentally different at low inhibitor levels, because in case (ii) some level of inhibitor addition can be tolerated without diminishing the overall (observed) respiration rate. In case (i) any level of inhibitor binding would, in theory, lower the observed rate.

When the inhibitor acts on the rate-limiting enzymatic reaction $d(e^-)/dt = \phi = k_1 E_{red}$, where $d(e^-)/dt$ is the rate of electron transport, E_{red} is the concentration of reduced enzyme (i.e., prepared to transfer an electron), and k_1 is the pseudo-first-order rate constant for electron transfer between successive carriers. We have assumed that electron transport from the active site is rate limiting. The same mathematical form would result if transport to the critical enzyme were rate limiting.

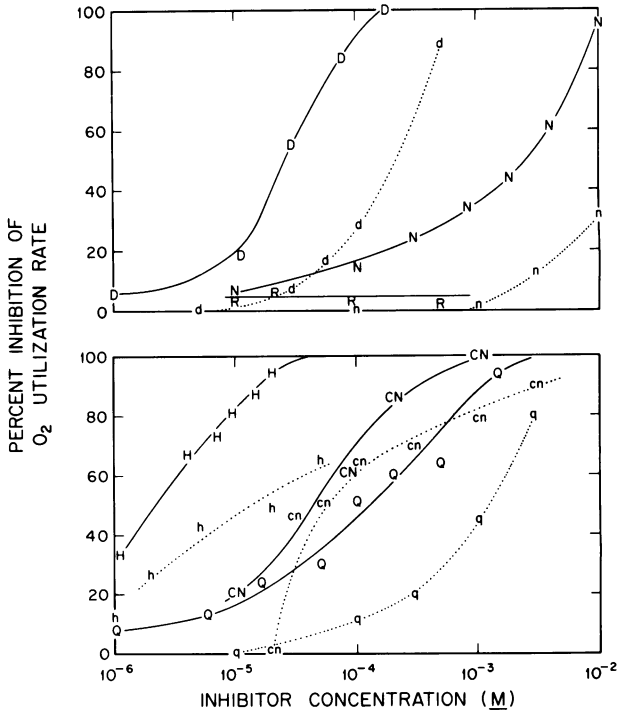

FIG. 3. Inhibition of electron transport to molecular oxygen as a function of inhibitor concentration in cultures of "*P. ferriductans*" (A_{600} = 0.10 cm^{-1} in uninduced experiments and 0.25 cm^{-1} in induced experiments.) Q,q, Quinacrine dihydrochloride; D,d, dicumarol; H,h, HOQNO; CN,cn, NaCN; N,n, NaN_3; R, rotenone. —— and uppercase letters, Cells grown at high O_2; - - - - and lowercase letters, cells grown at low O_2.

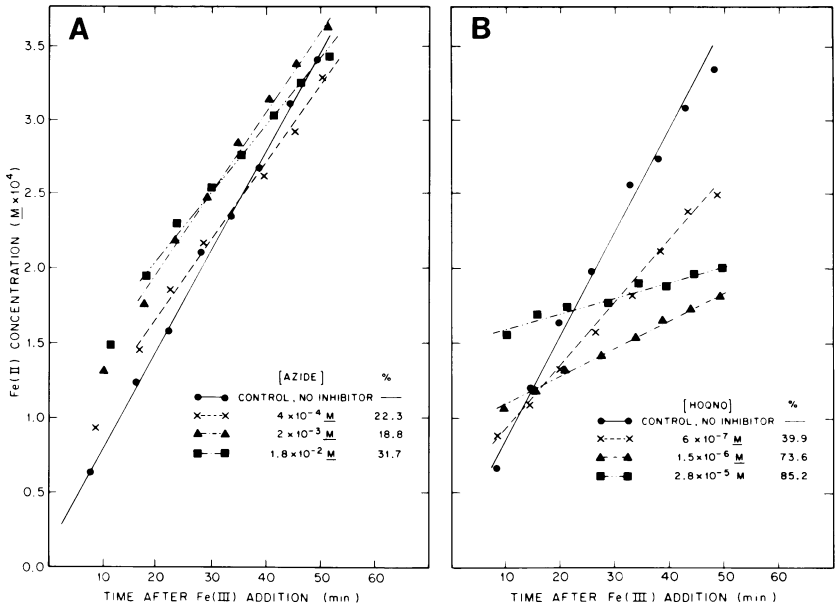

FIG. 4. (A) Inhibition of Fe(III) reduction by NaN_3 in uninduced cultures of "*P. ferrireductans*" (A_{600} = 0.25 cm^{-1}). Cells were grown at near-saturation O_2 levels. (B) Inhibition of Fe(III) reduction by HOQNO in uninduced cultures of "*P. ferrireductans*" (A_{600} = 0.25 cm^{-1}). Cells were grown at near-saturation O_2 levels.

In the presence of an inhibitor, a balance on the enzyme yields $E_T = E_{red} + E_{ox} + [EI]$, where E_T is the total enzyme concentration, E_{ox} is the concentration of the enzyme in its oxidized form, and [EI] is the concentration of enzyme-inhibitor complex (inactive enzyme). When electron transport is limited at this step, $E_{ox} \ll E_{red}$ and

$$E_T \cong E_{red} + [EI] \quad (1)$$

At equilibrium, the concentration of the enzyme bound to the inhibitor conforms to

$$K_I = [EI]/(E_{red} \cdot I) \quad (2)$$

where I is the bulk concentration of the inhibitor and K_I is the association constant for the enzyme and the inhibitor. Combining equations 1 and 2, we obtain $E_{red} \cong E_T/(1 + K_I \cdot I)$ and if $E_T = k_2\theta$, where θ is the cell density, then $\phi = k_3/(1 + K_I \cdot I)$ for experiments run at a single cell density. Note that K_I retains its physical significance and k_3 is a combination of physical constants ($k_1 \cdot k_2 \cdot \theta$).

By inverting both sides of equation 2 and multiplying by v_0, the uninhibited O_2 utilization rate is

$$\frac{v_0}{\phi} = \frac{v_0}{k_3} + \frac{v_0 K_I}{k_3} I \quad (3)$$

From equation 3, a plot of v_0/ϕ versus the inhibitor concentration (Fig. 7) yields estimates of v_0/k_3 (intercept) and K_I (slope/intercept). It should be noted that at high concentrations of inhibitors, which are known to interfere with electron transport to oxygen, transport past the site of inhibition is always rate limiting. Departures from the model predictions are expected at low inhibitor concentrations.

Fitted kinetic parameters are summarized in Table 2. When substituted back into equation 3, these permit the prediction of inhibitor efficiency as a function of concentration. Such predictions are compared with experimental observations for NaCN and quinacrine in Fig. 8. The results support the general validity of the model. The analysis was extended to inhibition by N_3^-, dicumarol, and HOQNO with similar results.

At high inhibitor concentrations, predictions of inhibitor efficiency were generally lower than observed inhibition rates, perhaps owing to secondary effects arising from a loss of cellular energy generation capacity. At low inhibitor concentrations, results were less consistent. When the model predictions are higher than the observations (e.g., inhibition by quinacrine), the inhibitor probably acts at a site which does not control the (uninhibited) rate of electron transport. Quinacrine and azide appeared to fit this pattern,

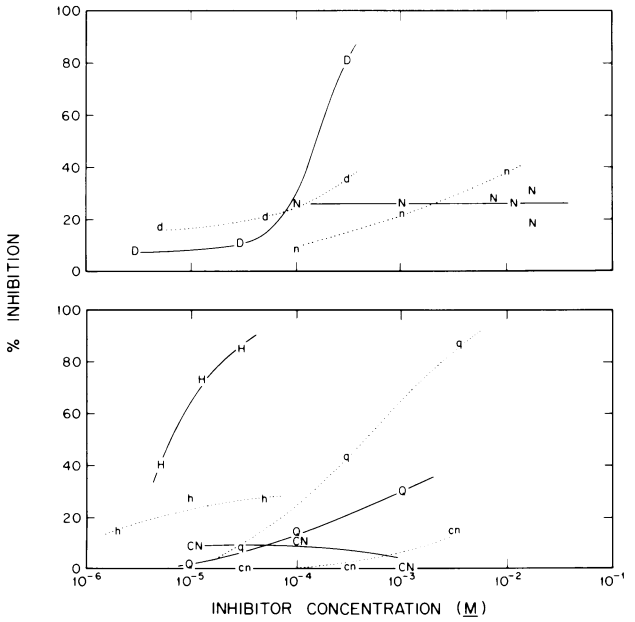

FIG. 5. Inhibition of electron transport to ferric iron as a function of the inhibitor concentration in cultures of "*P. ferrireductans*." (A_{600} = 0.25 cm^{-1} in all experiments.) Q,q, Quinacrine dihydrochloride; D,d, dicumarol; H,h, HOQNO; CN,cn, NaCN; N,n, NaN_3. —— and uppercase letters, cells grown at high O_2; - - - - and lowercase letters, cells grown at low O_2.

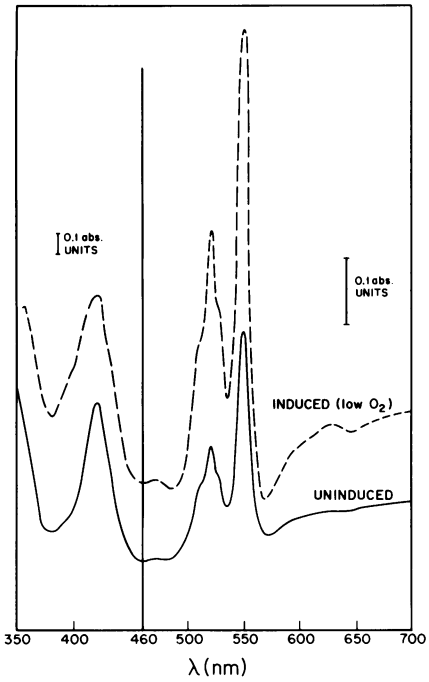

FIG. 6. Reduced-minus-oxidized spectra corresponding to induced and uninduced cultures of "*P. ferrireductans*." Cells were harvested at A_{600} = 0.75 cm^{-1}.

as indicated by v_0/k_3 values which exceed unity. Nothing more can be stated with confidence relative to the source of kinetic limits in the uninhibited case. However, because all intercept values are close to unity, we are encouraged to suspect that cellular production of electron transport chain components is well regulated, i.e., that no component is enormously overproduced or underproduced to the extent that it limits the uninhibited rate of electron transfer.

O_2 utilization in induced cells. In preliminary experiments (results not shown), it was observed that aerobic respiration capacity was significantly enhanced by prolonged growth at low oxygen tension. The enhancement could have resulted from the induction of branches within the electron transport

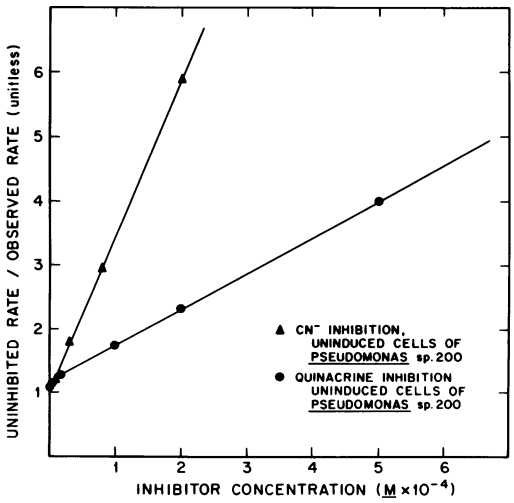

FIG. 7. Reciprocal rate of O_2 utilization (normalized) versus inhibitor concentration. The datum points are from the inhibition curves (Fig. 3). The slope-intercept information forms the basis of the parameter estimates summarized in Table 2.

TABLE 2. Summary of fitted kinetic parameters for inhibition of electron transport by respiratory poisons[a]

Inhibitor	v_0/k_3 (intercept, unitless)	K_I (slope/intercept, M^{-1})
Quinacrine dihydrochloride	1.2	4.6×10^3
Dicumarol	0.8	7.5×10^4
HOQNO	0.9	5.0×10^5
Sodium azide	1.2	2.9×10^2
Sodium cyanide	1.0	2.5×10^4

[a] The general model is given by equation 3 (see text for explanation). Intercept predictions higher than unity arose when low-level inhibitor additions were less effective than expected. It is likely that the active site of such inhibitors does not provide the ratelimiting step for uninhibited electron transport. Because none of the predictions is much greater than unity, it is probable that individual electron transport steps are kinetically in balance, i.e., that there is no severe bottleneck in the electron transport chain prior to inhibitor addition.

[b] Uninduced cells, A_{600} = 0.1 cm^{-1}.

chain, similar to the induction of an alternate cytochrome oxidase in *Escherichia coli* (5) and *Pseudomonas putida* (27). This hypothesis is supported by inhibition studies, which show that induced cells are less susceptible to inhibition by cyanide and azide than are cells grown at near-saturation oxygen levels. More direct evidence is provided by reduced-minus-oxidized spectra: reduced cytochrome *d* has a characteristic spectral peak near 632 nm; in its oxidized form it absorbs in the range 647 to 652 nm (24). Spectral characteristics induced under low oxygen tension (Fig. 6) are consistent with this pattern, offering evidence on behalf of an induced aerobic electron transport branch. Cytochrome *d* is relatively resistant to CN^- inhibition (24) owing to poor CN^- binding characteristics and provides competitive advantages under low-O_2 conditions (owing to a high O_2 affinity relative to other cytochrome oxidases).

A more detailed comparison of inhibition by cyanide versus HOQNO in cultures of "*P. ferrireductans*" grown at low oxygen tension is given in Fig. 9, which shows profiles of the O_2 utilization rate as a function of the oxygen concentration at several inhibitor concentrations. Although the respiration rate was sensitive to HOQNO concentration, the O_2 utilization rate was essentially a constant (independent of O_2 concentration in the range shown) at each inhibitor concentration. This would be expected when the inhibitor acts at a site other than cytochrome oxidase (i.e., transfer from cytochrome oxidase to O_2 is not rate limiting). In direct contrast, electron transport in the presence of cyanide was sensitive to oxygen concentration (Fig. 9B). At CN^- concentrations below 4 × 10^{-5} M, there was no apparent loss in

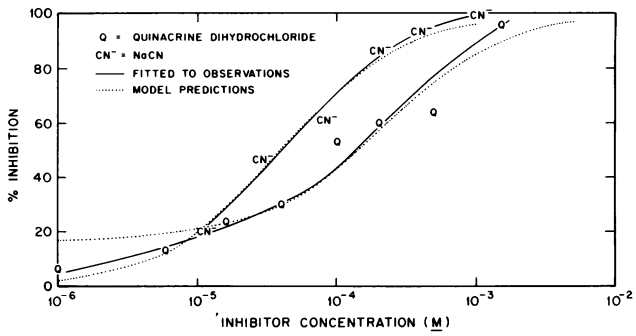

FIG. 8. Comparison of predicted and observed inhibition of aerobic respiration rates in (uninduced) cultures of "*P. ferrireductans*" (A_{600} = 0.10 cm^{-1}).

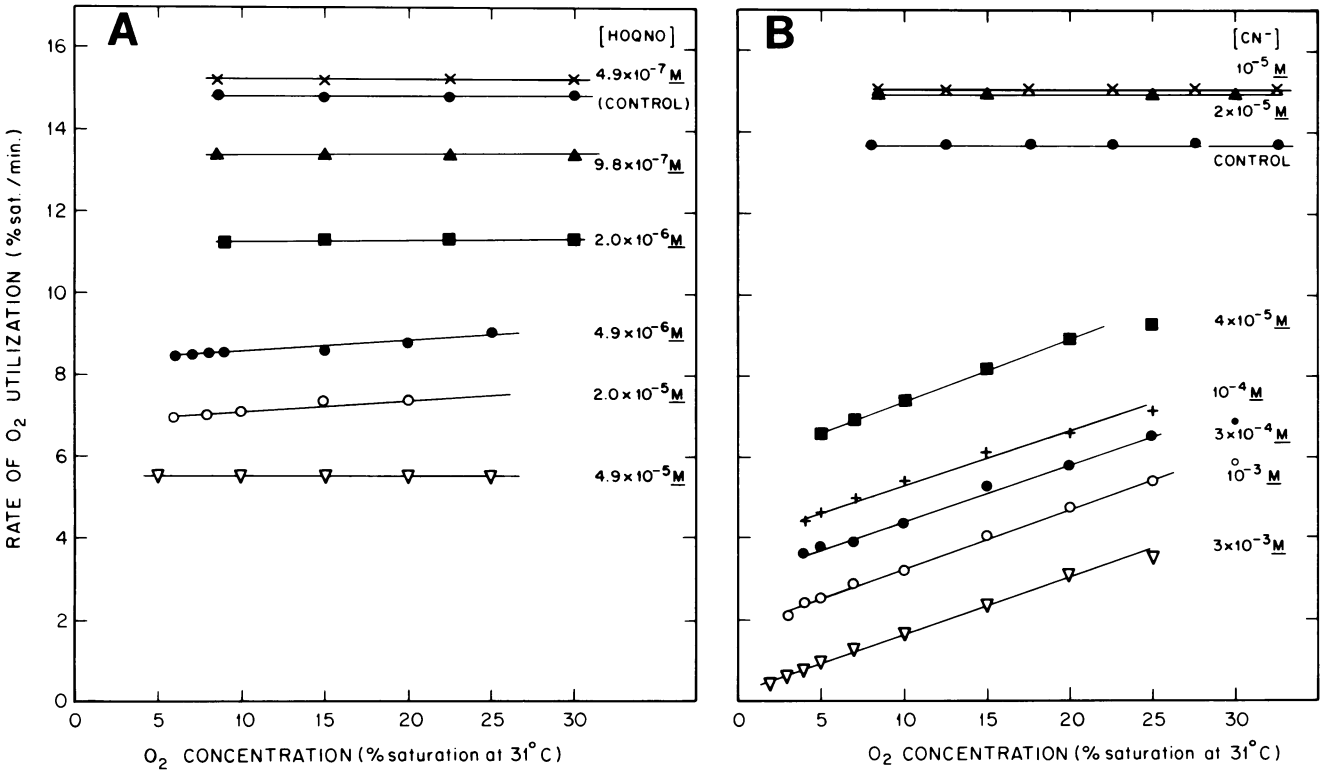

FIG. 9. (A) HOQNO inhibition of aerobic respiration in induced cultures of "*P. ferrireductans*" (A_{600} = 0.25 cm^{-1}). (B) Cyanide inhibition of aerobic respiration in induced cultures of "*P. ferrireductans*" (A_{600} = 0.25 cm^{-1}).

electron transport as a result of inhibitor addition, indicating that uninhibited respiration is not limited at the level of cytochrome oxidase. (This idea is supported by the lack of dependence of rate on O_2 concentration at low cyanide levels.) At higher inhibitor levels, a dependence on dissolved-oxygen concentration was evident. The similarity of the slopes for these curves suggests that the electron transport chain in these cells is branched. One of these branches was completely inhibited at cyanide levels approaching 3×10^{-3} M, whereas the other appeared to be less sensitive to CN^- inhibition (owing to either lower CN^- or higher O_2 affinity). Because uninduced cells were completely inhibited by 10^{-3} M CN^- (Fig. 3), it is possible that the branched chain develops in response to the low O_2 concentration. The enhancement of cytochrome *d* relative to other cytochrome oxidases has been observed in a variety of gram-negative heterotrophs in response to low O_2 or related conditions (24).

Differences in the susceptibilities of cytochrome oxidases to inhibition by CN^- or N_3^- can be explained as follows. The active site on one of the terminal oxidases could lie in a relatively hydrophobic region of the folded protein which excludes highly solvated CN^- [i.e., $CN(H_2O)_n^-$], while permitting the access of O_2 via diffusion. Alternatively, resistance could be conferred by a much higher affinity for O_2.

Other explanations for the data in Fig. 9 are possible. The slopes of the individual curves in Fig. 9B could result from time-dependent cyanide activity. Alternatively, one might postulate the existence of a single cytochrome oxidase whose electron transfer kinetics are affected by competitive cyanide binding in the available apical coordination site of an iron-porphyrin prosthetic group. The latter explanation would not account for complete cyanide inhibition among uninduced cells.

It is evident from Fig. 3 that respiratory inhibitors are less potent in cultures of induced cells than in their uninduced counterparts, perhaps owing to a general strengthening of the respiratory chain in cells grown at low oxygen tension. Augmentation of cytochrome densities in response to low O_2 conditions was evident in reduced-minus-oxidized spectra (Fig. 6). It is also possible that induction of parallel respiratory chain elements (branched chains) at low dissolved-oxygen concentrations accounts for the resistance to the inhibitors. Both quinacrine and dicumarol appeared capable of completely inhibiting respiration in both induced and uninduced cultures, perhaps because the transport chain branch points lie downstream from the sites of inhibition by these drugs.

In no case did DNP, an uncoupler of electron transport and oxidative phosphorylation, stimulate respiration. The acceleration of electron transport would be expected only if the transport kinetics were limited by the rate of dissipation of the proton motive force. Membrane distortion or steric interference due to DNP addition may be responsible for the observed inhibitory effect of the drug. The lack of dependence of inhibitory efficiency on cell number suggests that a low percentage of the added chemical is taken up by cells at DNP concentrations near 10^{-4} M.

Dissimilative iron reduction. Rates of dissimilative iron reduction in both induced and uninduced cultures of "*P. ferrireductans*" showed little dependence on cyanide or azide addition, suggesting that the terminal oxidase(s) for dissimilative iron reduction is not a cytochrome. Thermodynamic considerations indicate that dissimilative iron reduction is less energetically favorable than aerobic respiration (Arnold et al., in press). Thus, transport to ferric iron via an abbreviated electron transport chain is consistent with the results of both inhibitor studies and energetic calculations.

The induction of iron reduction capacity among cells

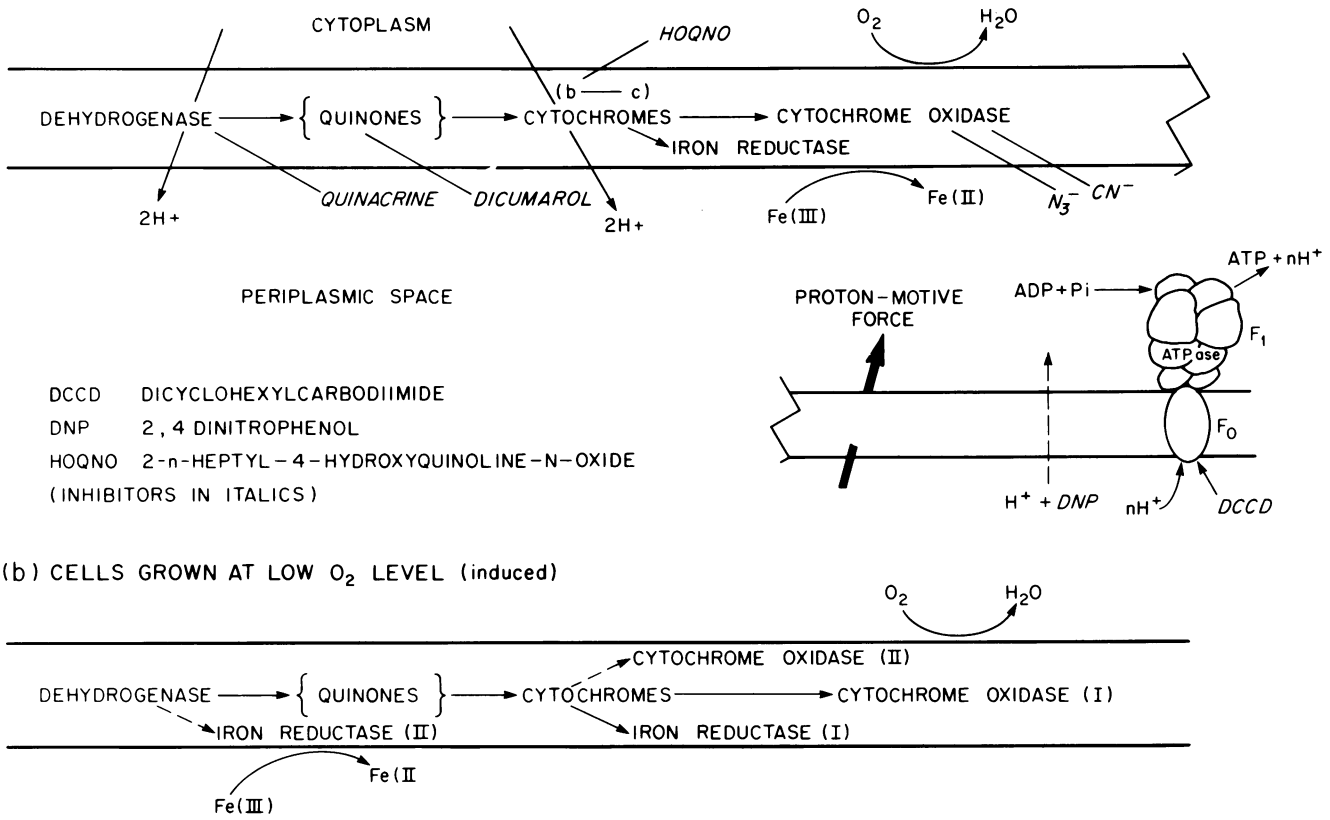

FIG. 10. Schematic representation of electron transport to O_2 or Fe(III) and transport inhibition in "*P. ferrireductans*." (a) O_2 utilization and iron reduction were both blocked by 10^{-4} M DCCD. DNP was a strong inhibitor of O_2 utilization. Fe(III) reduction was inhibited less efficiently. The order of inhibitor efficiency was as follows: (i) aerobic respiration, HOQNO > dicumarol $\cong$ CN^- > quinacrine > N_3^-; and (ii) iron reduction, HOQNO > dicumarol > quinacrine. N_3^- and CN^- were not effective inhibitors; CO inhibited completely. At A_{600} = 0.25 cm^{-1} (culture optical density) electron transport proceeded at (uninhibited) rates of 8×10^{-5} M e^- min^{-1} to O_2 and 9×10^{-6} M e^- min^{-1} to Fe(III). (b) - - -, Induced electron transport pathways. Iron reduction was unaffected by DCCD. The order of inhibitor efficiency was: (i) aerobic respiration, HOQNO > CN^- > dicumarol > quinacrine > N_3^-; (ii) iron reduction, only quinacrine had a major effect on electron transport at the concentrations tested. At A_{600} = 0.25 cm^{-1} (culture optical density) electron transport proceeded at (uninhibited) rates of 1.3×10^{-4} M e^- min^{-1} to O_2 and 6.6×10^{-5} *M* e^- min^{-1} to Fe(III).

grown at low oxygen tension (Fig. 1) has already been noted. Electron transport to Fe(III) in induced cells (A_{600} = 0.25 cm^{-1}) was six to eight times faster than iron reduction in similar, uninduced cultures. Thus, inhibitor efficiency curves by themselves (Fig. 5) do not permit the comparison of electron transport rates in induced and uninduced cultures. Nevertheless, inhibition studies support a qualitative picture of transport to Fe(III) in these cases. HOQNO, dicumarol, and carbon monoxide were effective inhibitors of iron reduction in cells grown at high oxygen tension but had only a minor impact on induced cultures. The implication is that cells grown at low oxygen concentrations transport electrons to Fe(III) via two branches. Because the induced path was not substantially affected by HOQNO or dicumarol, it may be considerably shorter than the constitutive branch (see Fig. 10). On the other hand, quinacrine, which was a more potent inhibitor in induced cells, appears to act on both pathways, ahead of the branch point present under low oxygen conditions. Because electron transport was more rapid in induced cells, quinacrine inhibition was more effective in such cultures.

A comparison of rates of electron transfer to O_2 and Fe(III) in uninduced cells indicated that anaerobic respiration is limited by ferrireductase activity. This limitation may disappear in induced cells. In such cultures (Fig. 1) it is evident that rates of electron transfer to Fe(III) can approach those of aerobic respiration.

Since DCCD inhibited electron transport in uninduced but not induced cells, oxidative phosphorylation is probably linked to iron reduction via the constitutive pathway only. This result supports the physical picture of an induced and constitutive branch for electron transfer to Fe(III). The more energetically favorable branch (constitutive) is linked to oxidative phosphorylation via proton translocation; the shorter (induced) branch serves only as a sink for cellular reducing power.

Conclusions. Taken together, inhibition data support the postulated mechanism for electron transport and inhibition in "*P. ferrireductans*" (Fig. 10). The differences in inhibition pattern and energetic considerations indicate that ferric iron is not reduced by a cytochrome oxidase in uninduced cells.

A second cytochrome oxidase and a second iron reductase were induced in "*P. ferrireductans*" by prolonged growth under low oxygen conditions. Induced cells could utilizeoxygen somewhat faster than could their uninduced counterparts. Iron reduction by induced cells was almost 1 order of magnitude faster than measured rates in uninduced cultures.

Although the constitutive iron reductase in "*P. ferrireductans*" was completely inhibited by 10^{-4} M DCCD after 60 min, the induced system was unaffected. Iron reduction by the induced system is probably not linked to oxidative phosphorylation, whereas the constitutive iron reductase does drive ATP synthesis.

Because electron transfer to dissolved oxygen is apparently more rapid than to Fe(III) among uninduced cells, we conclude that iron reduction is limited kinetically at the level of Fe(III) reductase. When dissolved oxygen was the electron acceptor, the interpretation is less clear. Our analysis indicates that neither azide nor quinacrine acted at the rate-limiting site in uninduced cells. Several potential control points remain along the postulated transport chain; control could also reside with metabolic processes ahead of the electron transport chain or in limits imposed by dissipation of the transmembrane proton motive force. Because respiration was not accelerated by DNP (uncoupler) addition, control by the proton motive force seems less likely.

Striking differences in inhibition patterns (and electron transport chain configurations) between induced and uninduced cells are related to the dissolved oxygen level in the growth medium. The importance of controlling environmental variables while investigating bacterial metabolism and energetics is apparent.

ACKNOWLEDGMENTS

We are grateful to D. W. S. Westlake of the Department of Microbiology, University of Alberta, Edmonton, Alberta, Canada, for generously providing the microorganism used in this study, *Pseudomonas* sp. strain 200. The taxonomic studies leading to species identification were undertaken and reported by D. Westlake and C. O. Obuekwe; we have changed its name to "*Pseudomonas ferrireductans*" (upon request of a reviewer) with some reluctance. We hope that its new name will provide the microorganism with deserved distinction without causing excessive confusion. We appreciate the support and encouragement of Ryszard Gajewski and Duane L. Barney. We thank Sandy Brooks, Elaine Granger, and Nancy Tomer of the Caltech Environmental Sciences and Engineering staff for secretarial and drafting assistance during manuscript preparation.

This work was supported by U.S. Department of Energy contract no. DE-AS03-83ER13125 administered within the Division of Advanced Energy Projects, Office of the Basic Energy Sciences.

LITERATURE CITED

1. **American Public Health Association.** 1985. Standard methods for the examination of water and wastewater, 16th ed, p. 215–220. American Public Health Association, Washington, D.C.
2. **Brock, T. D., and J. Gustafson.** 1976. Ferric iron reduction by sulfur- and iron-oxidizing bacteria. Appl. Environ. Microbiol. **32**:567–571.
3. **Futai, M., and H. Kanazawa.** 1983. Structure and function of proton-translocating adenosine triphosphatase (F_0F_1): biochemical and molecular biological approaches. Microbiol. Rev. **47**:285–312.
4. **Ghiorse, W. C., and H. L. Ehrlich.** 1976. Electron transport components of the MnO_2 reductase system and the location of the terminal reductase in a marine *Bacillus*. Appl. Environ. Microbiol. **31**:977–985.
5. **Haddock, B. A., and C. W. Jones.** 1977. Bacterial respiration. Bacteriol. Rev. **41**:47–99.
6. **Harold, F. M.** 1970. Antimicrobial agents and membrane function. Adv. Microb. Physiol. **4**:45–104.
7. **Heinen, W.** 1971. Inhibitors of electron transport and oxidative phosphorylation, p. 383–393. *In* J. R. Norris and D. W. Ribbons (ed.), Methods in microbiology, vol. 6A. Academic Press, Inc., New York.
8. **Hewitt, E. J., and D. J. D. Nicholas.** 1963. Cations and anions: inhibitions and interactions in metabolism and in enzyme activity, p. 311–427. *In* R. M. Hochster and J. H. Quastel (ed.), Metabolic inhibitors: a comprehensive treatise, vol. 2, Academic Press, Inc., New York.
9. **Hinkle, P. C., and R. E. McCarty.** 1978. How cells make ATP. Sci. Am. **228(3)**:104–123.
10. **Jones, C. W.** 1983. Bacterial respiration and photosynthesis. Aspects Microbiol. **5**:38–58.
11. **Kashket, E. R.** 1982. Stoichiometry of the H^+-ATPase of growing and resting, aerobic *Escherichia coli*. Biochemistry **21**:5534–5538.
12. **Kino, K., and S. Usami.** 1982. Biological reduction of ferric iron by iron- and sulfur-oxidizing bacteria. Agric. Biol. Chem. **46**:803–805.
13. **Kurimura, Y., R. Ochiai, and N. Matsuura.** 1968. Oxygen oxidation of ferrous ions induced by chelation. Bull. Chem. Soc. Jpn. **41**:2234–2239.
14. **Lemberg, R., and J. Barrett.** 1973. Cytochromes. Academic Press, Inc., New York.
15. **McLaughlin, S.** 1972. The mechanism of action of DNP on phospholipid bilayer membranes. J. Membr. Biol. **9**:361–372.
16. **Mitchell, P.** 1961. Coupling of phosphorylation to electron and hydrogen transfer by a chemi-osmotic type of mechanism. Nature (London) **191**:144–148.
17. **Mitchell, P.** 1966. Chemiosmotic coupling in oxidative and photosynthetic phosphorylation. Biol. Rev. Camb. Philos. Soc. **41**:445–502.
18. **Mitchell, P., and J. Moyle.** 1967. Acid-base titration across the membrane system of rat-liver mitochondria. Catalysis by uncouplers. Biochem. J. **104**:588–599.
19. **Munch, J. C., and J. C. G. Ottow.** 1983. Reductive transformation mechanism of ferric oxides in hydromorphic soils. Ecol. Bull.-NFR (Naturvetensk-Forskningsradet) **35**:383–394.
20. **Obuekwe, C. O., and D. W. S. Westlake.** 1982. Effects of medium composition on cell pigmentation, cytochrome content, and ferric iron reduction in a *Pseudomonas* sp. isolated from crude oil. Can. J. Microbiol. **28**:989–992.
21. **Obuekwe, C. O., D. W. S. Westlake, and F. D. Cook.** 1981. Effect of nitrate ion on reduction of ferric iron by a bacterium isolated from crude oil. Can. J. Microbiol. **27**:692–697.
22. **Pestka, S.** 1975. Chloramphenicol. Antibiotics **3**:370–395.
23. **Pongs, O.** 1979. Chloramphenicol. Antibiotics **5(1)**:26–42.
24. **Poole, R. K.** 1983. Bacterial cytochrome oxidases a structurally and functionally diverse group of electron-transfer proteins. Biochem. Biophys. Acta **726**:205–243.
25. **Smith, L.** 1968. The respiratory chain system of bacteria, p. 55–122. *In* T. P. Singer (ed.), Biological oxidations. John Wiley & Sons, Inc., New York.
26. **Stryer, L.** 1981. Biochemistry, p. 307–329. W. H. Freeman & Co., San Francisco.
27. **Sweet, W. J., and J. A. Peterson.** 1978. Changes in cytochrome content and electron transport patterns in *Pseudomonas putida* as a function of growth phase. J. Bacteriol. **133**:217–224.
28. **Tamura, H., K. Goto, T. Yotsuyanagi, and M. Nagayama.** 1974. Spectrophotometric determination of iron(II) with 1,10-phenanthroline in the presence of large amounts of iron(III). Talanta **21**:314–318.
29. **Troshanov, E. P.** 1968. Iron- and manganese-reducing microorganisms in ore-containing lakes of the Karelian Isthmus. Mikrobiologiya **37**:934–940.
30. **Troshanov, E. P.** 1969. Conditions affecting the reduction of iron and manganese by bacteria in the ore-bearing lakes of the Karelian Isthmus. Mikrobiologiya **38**:634–643.
31. **White, D. C., and P. R. Sinclair.** 1971. Branched electron-transport systems in bacteria. Adv. Microb. Physiol. **5**:173–211.
32. **Wolfe, A. D.** 1975. Quinacrine and other acridines. Antibiotics **3**:203–233.
33. **Wright, C. I., and J. C. Sabine.** 1944. The effect of atabrine on the oxygen consumption of tissues. J. Biol. Chem. **155**:315–320.